

Study of interaction between fluorescent dyes and Cucurbituril host in aqueous solution

A thesis submitted to

Indian Institute of Science Education and Research Pune

in partial fulfillment of the requirements for the

BS-MS Dual Degree Programme

Thesis Supervisor: Dr. Partha Hazra

By

Anup Ingole

April, 2013



Indian Institute of Science Education and Research Pune

Sai Trinity Building, Pashan, Pune India 411021.

Certificate

This is to certify that this thesis entitled "Study of interaction between fluorescent dyes and Cucurbituril host in aqueous solution" submitted towards the partial fulfillment of the BS-MS dual degree program at the Indian Institute of Science Education and Research Pune, represents work carried out by Mr. Anup Ingole under the supervision of Dr. Partha Hazra.

Date:

Place:

Signature

Declaration

I hereby declare that the matter embodied in the report entitled “Study of interaction between fluorescent dyes and Cucurbituril host in aqueous solution” are the results of the investigations carried out by me at the Department of Indian Institute of Science Education and Research, Pune, under the supervision of Dr. Partha Hazra and the same has not been submitted elsewhere for any other degree.

Date:

Place:

Signature

Dedicated to my Father

Acknowledgements

I would like to thank, Dr. Partha Hazra for giving me an opportunity to do research project and also for his valuable suggestions. I am very thankful to my lab colleague Mr. Krishna Gavvala for his support and guidance. I am also thankful to Abhigyan, Hrishikesh and Rajkumar for their cooperation and advices. I am grateful to Director, IISER-Pune for providing excellent experimental facilities. I am thankful to DST for inspired fellowship.

Contents

1. INTRODUCTION	P9
2. METHODS	P13
3.1. STUDY OF INTERACTION BETWEEN PRODAN AND CUCURBITURIL	P15
3.2. STUDY OF INTERACTION BETWEEN BIPYRIDINE DIOL [BP(OH) ₂] AND CUCURBITURIL.....	P22
3.3. STUDY OF INTERACTION BETWEEN HPTS and CUCURBITURIL	P29
4. CONCLUSIONS	P34
REFERENCES	

List of Figures

1. **Fig.1** Absorption spectra of PRODAN in different concentration of (a) CB6, (b) CB7, (c) CB8.....P16
2. **Fig.2** Fluorescence spectra of PRODAN in different concentration of (a) CB6, (b) CB7, (c) CB8, $\lambda_{ex}=355$ nm.....P17
3. **Fig.3** Fluorescence spectra of PRODAN in different pH, $\lambda_{ex}=355$ nm.....P18
4. **Fig.4** Fluorescence decay parameters of PRODAN in water and in different concentration of (a) CB7, and (b) CB8, $\lambda_{ex}=375$ nm.....P19
5. **Fig.5** Fluorescence anisotropy decay parameters of PRODAN in water and in different concentration of (a) CB7, and (b) CB8, $\lambda_{ex}=375$ nm.....P19
6. **Fig.6** Proposed structure of PRODAN: CBn complex.....P21
7. **Fig.7** Absorption spectra of BP(OH)₂ in different concentration of (a) CB6, (b) CB7, (c) CB8.....P23
8. **Fig.8** Fluorescence spectra of BP(OH)₂ in different concentration of CB6, CB7 and CB8, $\lambda_{ex}=345$ nm.....P25
9. **Fig.9** Fluorescence spectra of BP(OH)₂ in different concentration of CB6, CB7 and CB8, $\lambda_{ex}=425$ nm.....P25
10. **Fig.10** BH plots of BP(OH)₂ in (a) CB7, and (b) CB8.....P26
11. **Fig.11** Fluorescence decay parameters of BP(OH)₂ in water and in different concentration of (a) CB6, (b) CB7, (c) CB8, $\lambda_{ex}=375$ nm.....P26
12. **Fig.12** Fluorescence anisotropy decay parameters of BP(OH)₂ in water and in different concentration of CB6, CB7, and CB8, $\lambda_{ex}=375$ nm.....P27
13. **Fig.13** Structure of the most stable minimum configuration of BP(OH)₂ embedded inside the CB7 cavity.....P28
14. **Fig.14** Structure of the most stable minimum configuration of BP(OH)₂ embedded inside the CB8 cavity.....P28
15. **Fig.15** Absorption spectra of HPTS in different concentration of CB8.....P30
16. **Fig.16** Fluorescence spectra of HPTS in different concentration of CB8, (a) $\lambda_{ex}=405$ nm, and (b) $\lambda_{ex}=455$ nm.....P31

17. Fig.17 BH plot of HPTS in CB8.....	P31
18. Fig.18 Fluorescence Decay parameters of HPTS in different concentration of CB8, $\lambda_{ex}=375$ nm.....	P32
19. Fig.19 Fluorescence Anisotropy Decay parameters of HPTS in water and in 100 μ M concentration of CB8, $\lambda_{ex}=375$ nm.....	P32
20. Fig.20 Structure of the most stable minimum configuration of HPTS embedded inside the CB8 cavity.....	P33

List of Tables

1. Table 1 Fluorescence Lifetime decay parameters of PRODAN in different CB7 concentration, $\lambda_{ex}=375$ nm.....	P20
2. Table 2 Fluorescence Lifetime decay parameters of PRODAN in different CB8 concentration, $\lambda_{ex}=375$ nm.....	P20
3. Table 3 Fluorescence anisotropy decay parameters of PRODAN in different CB8 concentration, $\lambda_{ex}=375$ nm.....	P20
4. Table 4 Fluorescence Lifetime decay parameters of BP(OH) ₂ in water, CB6, CB7, and CB8, $\lambda_{ex}=375$ nm.....	P27
5. Table 5 Fluorescence anisotropy decay parameters of BP(OH) ₂ in water, CB6, CB7, and CB8, $\lambda_{ex}=375$ nm	P28
6. Table 6 Fluorescence Lifetime decay parameters of HPTS in different concentration of CB8 aqueous solution, $\lambda_{ex}=375$ nm	P32

Abstract

Study of interaction between fluorescent dyes and Cucurbituril host in aqueous solution

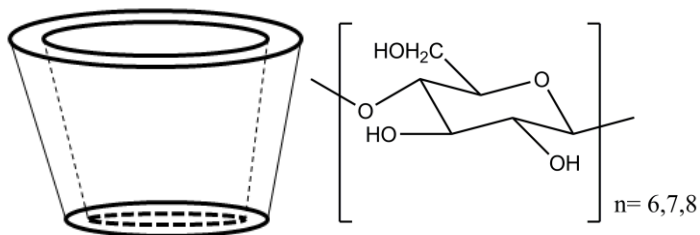
The photophysics of PRODAN (6-propionyl-2-dimethylaminonaphthalene), BP(OH)₂ (2,2'-bipyridine-3,3'-diol), and HPTS (8-hydroxypyrene-1,3,6-trisulfonate, pyranine) guest molecules have been studied in cucurbiturils (CB_n, where n=6-8) having different cavity sizes. Cucurbituril has interior hydrophobic cavity and hydrophilic carbonyl groups present at its portal. It has been observed that fluorescence intensity of PRODAN is quenched upon encapsulation by CB_n cavity. The restriction of intramolecular charge transfer (ICT) within PRODAN inside the CB_n cavity causes the quenching of fluorescence. In CB cavity due to higher shift of pK_a value, dimethylamino group is getting protonated which causes the restraint of ICT. BP(OH)₂ exists in two forms, one di-enol (DE) form in the ground state and other di-zwitterion (DZ) form in the excited state after intramolecular double-proton transfer. DZ form exists in the ground state exclusively in water. Binding of BP(OH)₂ to CBs was studied by following the changes in its absorption and fluorescence spectra after addition of CBs. It was found that inclusion of BP(OH)₂ inside CB7 and CB8 causes enhancement in fluorescence intensity. The spectral behavior of HPTS is studied in CB8 using absorption, steady state emission and time-resolved emission techniques. It has been observed that the absorption and fluorescence intensity of HPTS is getting reduced due to hydrogen bonding between -OH group of HPTS and carbonyl groups of CBs. The lifetime measurement values also decreases as CB8 concentration increases.

1. Introduction

The fluorescence property of an organic dye depends strongly on the local environment.¹ Fluorescent dyes have been used as molecular probe not only to determine micro environmental parameters, such as the polarity of media, but also to study their relocation and distribution dynamics in micro heterogeneous systems such as micelles, membranes, polymers, interfaces, cellular media and even in discrete supramolecular systems.^{2,3} Fluorescence properties of the molecules can be used to monitor the formation of host/guest complexes with various macrocyclic hosts and the encapsulation of the dye into their hydrophobic cavity can be used to probe the microenvironment of the host.⁴ There are mainly three types of water soluble supramolecular hosts which are discussed below. The present study focuses on these organic macrocycles and fluorescent guests with the perspective of using them for potential biological and environmental applications in the areas of sensing and signaling.

(i) Cyclodextrins

Cyclodextrins (CD), α -, β -, and γ -CD, are cyclic oligomers composed of 6, 7, and 8 α -D-glucose units respectively.⁴ They possess a uncharged hydrophobic inner cavity and hydroxyl group rim, which provides additional hydrogen bonding motifs for



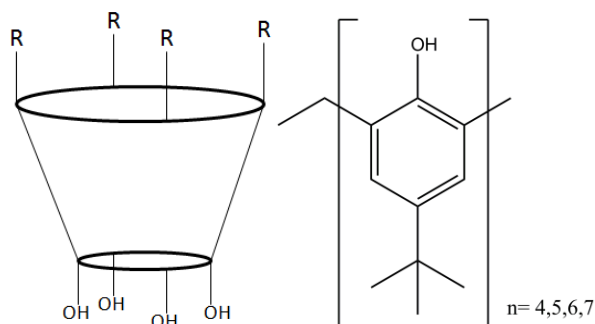
Scheme 1: Cyclodextrin

the binding of organic guests. Their commonly shaped as truncated cone or, sometimes visualized as a molecular cup (Scheme 1). Out of three different sizes of (6, 7, 8) CD, the medium sized β -CD can encapsulate a variety of small organic residues e.g. aryl groups, and sometimes bulkier ones like adamantane.⁵ It is unfortunately also the least water-soluble derivative (16mM). The smaller and larger homologues (α -CD and γ -CD) are though more water soluble (150 and 180 mM, respectively), have a too small or too large cavity to ensure strong binding. Depending upon the structure of the guests,

cyclodextrins are able to form host-guest complexes with different hydrophobic organic molecules. Therefore, these molecules have so many applications in different fields. Cyclodextrins have been used as a potential drug carrier in drug delivery systems. In food applications, α -cyclodextrins have been used as weight loss supplements as an alternative to other anti-obesity medications.⁶

(ii) Calix[n]arenes

The calixarene macrocycle is built up by base-catalyzed condensation of 4-substituted phenols with formaldehyde. The electron rich hydroxyl or alkoxy substituted aryl rings act as electron donors toward excited states (Scheme 2), which causes fluorescence quenching upon binding of fluorescent dyes.⁷ The calixarenes are available in different sizes (CX4, CX5, CX6 and CX8). The smallest homologue, CX4, is typically represented as a truncated cone or cup. The conformational variety of calixarenes is much larger than that of cyclodextrins and is the major drawback to use them in supramolecular chemistry. For application purpose, calixarenes have been used in polymer synthesis. It is employed as an efficient catalyst for the polymerization of styrene, ethylene, propylene oxide, butadiene, styrene oxide and trimethylene carbonate.⁸

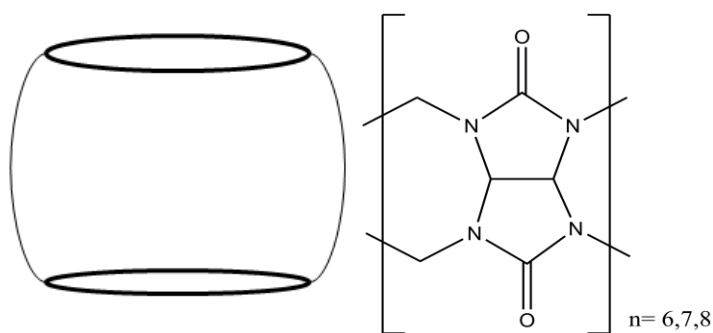


Scheme 2: Calix[n]arene

(iii) Cucurbiturils

Initially discovered by Behrend in 1905,⁹ they are obtained by acid-catalyzed condensation of glycoluril with formaldehyde under carefully controlled conditions. Depending on the number of glycoluril units, different homologue sizes are known, prominently CB6, CB7, and CB8 with their cavity size of 3.9Å, 5.4Å and 6.9Å respectively. All CBs have a highly symmetrical, pumpkin-shaped structure (Scheme 3) with two identical portals and an interior hydrophobic cavity, akin to cyclodextrins and calixarenes in their cone conformation. The even numbered homologues display a low

water-solubility, which is nevertheless sufficient to study their complexation with many fluorescent dyes. Among the odd-numbered, water-soluble homologues, CB5 is too small to interact with fluorescent dyes. However, CB7 displays a favorable combination of a sufficient cavity size and high water solubility (5 mM), which turns it into the most promising cucurbituril host for binding of fluorescent dyes. While the hydrophobic interior provides a potential inclusion site for nonpolar molecules, the polar carbonyl at the portals allows the cucurbiturils to bind ions and charged molecules through charge-dipole and hydrogen bonding interactions.¹⁰ In recent years, CBs have been established as versatile and interesting host molecules, which form stable inclusion complexes with small guest molecules such as organic dyes, metal ions, and protonated alkyl and arylamines. Although the guest binding properties of cucurbiturils in solution are being studied using NMR spectroscopy, calorimetry, and UV-absorption spectroscopy,¹¹ very little is known about the effect of CBs on the photophysical and photochemical behavior of fluorophores and in particular common fluorescent dyes. Recently, this class of macrocycles has been shown to exhibit low in vivo as well as in vitro toxicity, thereby facilitates biologically relevant applications.¹²



Scheme 3: Cucurbituril

Macrocycle-dye interaction

The inclusion of the fluorescent dyes can affect their photophysical properties and potentially lead to unprecedented effects and, ultimately, new applications. Numerous studies are dealing with the changes of fluorescent properties upon complexation.⁴ Let us first discuss the different photophysical pathways which could be potentially altered by macrocyclic complexation or confinement in general. When the molecule is excited to the first singlet-excited state, several pathways of deactivation apply, including radiative decay (k_r), Forster resonance energy transfer (k_{FRET}), photoproduct formation (k_p), internal conversion (k_{IC}), intersystem crossing (k_{ISC}),

solvent-induced quenching, and quenching by additives or oxygen. Upon host-guest complexation, the fluorescence can be either quenched or enhanced depending upon their interaction in the excited state.

In most of the cases, the effects of inclusion complexation can be understood in related to either the change in location of the fluorescent dye into the more hydrophobic environment of the host cavities or the geometrical confinement of the chromophore within the host, which restricts rotational and vibrational freedom, thereby disfavoring nonradiative decay pathways. After complex formation, the fluorophore might also be “mechanically” protected from external (intermolecular) quenchers, including the solvent and oxygen, by the walls of macrocycles.¹³ The interaction between solvent molecules and an excited dye leads to proton or hydrogen transfer reactions and it can promote single or multiphoton ionization processes, which can lead to a permanent depletion of the chromophore by irreversible chemical follow-up reactions unless the ground states are efficiently recovered by conical intersections along the reaction pathway.¹⁴ Due to formation of inclusion complex, dye aggregation may also be hindered, leading to notable changes in the photophysical properties of the dye containing solution. On the other hand, the formation of dimers may be promoted by hosts with larger cavities (e.g., CB8). Furthermore, interaction between host and dye molecules at the portal (association rather than encapsulation) can lead to changes in fluorescence via host-mediated dye aggregates near the portals of the macrocycles.¹⁵ Apart from photophysical effects on the fluorescent dyes caused by confinement, microenvironmental changes, and diffusional quenching, changes in chemical equilibria, particularly protonation equilibria, can also be observed. For example, cucurbiturils cause pKa shift towards higher values in the ground as well as the excited state.¹⁶

In the present work, we have studied fluorescent behavior of PRODAN, Bipyridine Diol (BP(OH)₂), and HPTS molecules in different sizes of cucurbiturils (CB6, CB7 & CB8). Finally, release of the dye has been achieved by using simple external stimulus like NaCl.

2. METHODS

2.1. Experimental Section.

PRODAN, BP(OH)₂, HPTS and all other solvents were obtained from Sigma Aldrich. All the solutions were prepared in millipore water.

PRODAN in MeOH stock solution was dissolved in 2.5 ml water and then CB6 was added gradually to the stock solution till 50 μM , CB7 was added till 500 μM , and CB8 was added till 100 μM .

Bipyridine Diol in MeOH stock (10 μl) was prepared to get dissolved in 2.5 ml of water. In this solution CB6 (in water) was added gradually till 50 μM , CB7 addition till 1100 μM , and CB8 addition till 100 μM concentration.

For HPTS, instead of water we used PBS buffer of pH 7.4 to stabilize SO₃⁻ (acidic) groups so that pH of solution will not get changed. In this HPTS buffer solution, CB8 was added gradually till 100 μM concentration.

The steady-state absorptions were recorded by Evolution 300 UV–Visible spectrophotometer (Thermo Fisher Scientific) and emission spectra were measured using a Fluorolog-3 (Horiba Jobin Yvon). All the steady state and time-resolved measurements were done at room temperature (298 ± 1 K). Fluorescence decays were collected by time correlated single photon counting technique (TCSPC) setup (Horiba Jobin Yvon). As a sample excitation source, we have used 405 nm diode Laser (IBH, UK, NanoLED-405L) having a FWHM of 89 ps. The fluorescence signals were collected in magic angle using a MCP-PMT (Hamamatsu, Japan) detector. For time resolved anisotropy study we have used motorized polarizer in the emission side. The analysis of lifetime and anisotropy data was done by IBH DAS6 analysis software. We have fitted both lifetime as well as anisotropy data with a minimum number of exponential. We have performed the experiment two times to get correct measurements.

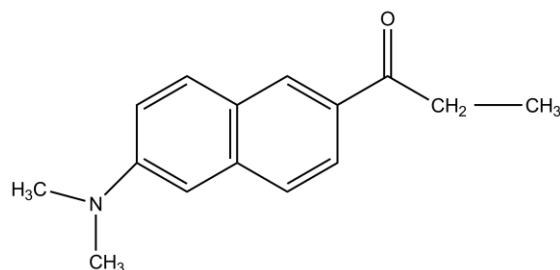
2.2. Computational Section.

The molecular docking study was performed by means of the AutoDock 4.2 software package using Auto Dock Tools 1.5.4 (ADT). Polar hydrogen atoms and Kollman charges were added to the input files. The binding site on the macromolecule was defined by using Auto Grid with 60x60x60 grid points and a grid space of 0.375 Å. The Lamarckian Genetic Algorithm (LGA) with a local search was used as a search method. On the basis of LGA, a total of 100 runs for each ligand were performed with a population size of 150. Docking analysis was performed by using the cluster of a root-mean-square deviation (rmsd) of 2.0 Å. During docking, the host (CB7) was kept rigid and the guest molecules (BP(OH)₂ and HPTS) were flexible. The docking results were analyzed and visualized by using ADT. After 100 runs, the best conformer was ranked according to the docking energy and geometry matching.

3.1. STUDY OF INTERACTION BETWEEN PRODAN AND CUCURBITURIL

Fluorescent molecules which are sensitive to environmental polarities have been extensively used as molecular probes in studies of physicochemical properties of solvents, surfaces, proteins, membranes, cells, etc.¹⁷⁻¹⁹

PRODAN (6-propionyl-2-dimethyaminonaphthalene) (Scheme 4), lipophilic fluorescent probe, first synthesized and characterized by Weber and Farrisin 1979,²⁰ has been mainly used in



Scheme 4: PRODAN

investigation of physical and chemical properties of membranes and biological macromolecules. Its absorption and emission are strongly dependent upon the environmental polarity.²⁰

Depending upon local polarity PRODAN shows fluorescence, one at 435 nm and the other at 530 nm from less polar and more polar excited states, respectively.²¹ Fluorescence at 435 nm is due to locally excited (LE) state and the polarity dependent fluorescence (at 530 nm) is attributed to an intramolecular charge transfer (ICT) excited state.^{20,21} PRODAN possesses an electron-donating dimethylamino group and the electron withdrawing propionyl group which is positioned at maximal distance from the amino group. Transfer of charge from the dimethylamino (donor) group to the propionyl (acceptor) group produces a substantial excited state dipole moment which is sensitive to the polarity of the medium. This change in dipole moment causes its large Stokes shift (i.e. from 435nm to 530nm).²¹ Bunker et al.²² have determined the excited-state dipole moment of PRODAN which is equal to 10 D and suggested that solvent-specific interactions (e.g. hydrogen bonding) may cause a large Stokes shift in polar protic solvents. Recently, Samanta et al.²³ have suggested this value to be 4.4-5.0 D based on transient dielectric loss measurements.

Jacob and co-workers²⁴ have studied fluorescence of PRODAN from the locally excited (LE) and charge transferred (CT) states in the heterogeneous

environment provided by reverse micelles formed by sodium 1,4-bis-(2-ethylhexyl) sulfosuccinate (AOT)/*n*-heptane/water. They have found that the LE and CT states of PRODAN solvate on different time scales in reverse micelles (2 and 0.4 ns, respectively), and have concluded that PRODAN can be used to probe the heterogeneous environments.

Al-Hassan et al.²¹ have studied the fluorescence emission of PRODAN in different sizes of cyclodextrin (α , β , and γ -CD). They have shown that in either α -CD or β -CD PRODAN emits a single fluorescence band at 525 and 510 nm, respectively. But when it dissolved in γ -cyclodextrin (CD) aqueous solutions it showed two bands which were found to depend on time and temperature. It is the direction of the dimethylamino group of PRODAN (toward the smaller rim or toward the large rim of the γ -CD cavity) that governs the generation of two kinds of fluorescence, a less polar, 435 nm and a more polar, 510 nm observed for PRODAN in γ -CD aqueous solutions. Cyclodextrin has hydrophobic cavity with no charge on it. Our main aim was to study the modulation of photophysical properties of PRODAN inside cucurbiturils which has hydrophobic cavity as well as hydrophilic carbonyl groups at its portal. We found that ICT emission of PRODAN is quenched in presence of CBs. The extent of quenching was found to be more in case of CB7. We concluded that the main reason for this quenching may be due to ion-dipole interactions accounts for the pKa shift towards higher values, which reflects the increased stability of the protonated dye in the complex.

RESULTS AND DISCUSSION

Absorption study: Absorption spectra of PRODAN in water as well as in different sizes

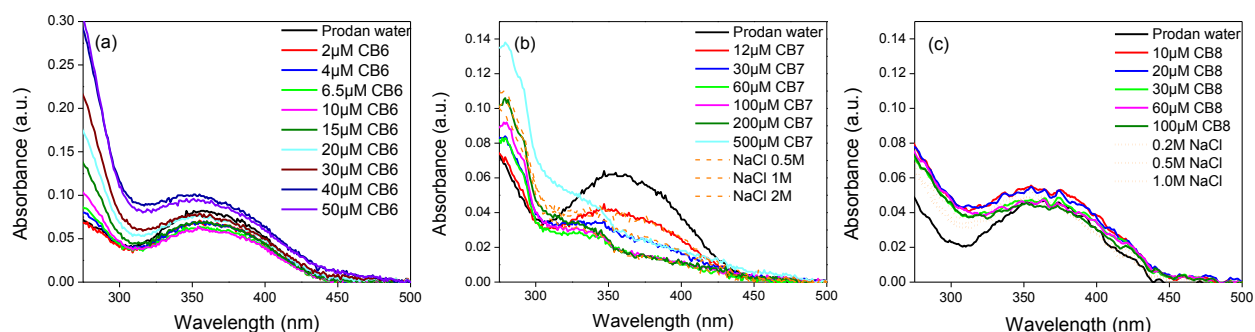


Fig.1 Absorption spectra of PRODAN in different concentration of (a) CB6, (b) CB7, and (c) CB8.

of cucurbituril (CB6, CB7, and CB8) aqueous solutions are shown in Fig.1. PRODAN shows absorption peak at 355 nm in aqueous solution. In presence of CB6 aqueous, there is no considerable change in the absorption peak. It may be attributed to the small cavity size of CB6 and hence there may be no strong interaction between PRODAN and CB6. In CB7 aqueous solution, the absorbance of PRODAN reduces as CB7 concentration increases. This can be attributed to strong interaction between PRODAN and CB7. For CB8 aqueous solutions, there is no considerable change in absorbance of PRODAN. The reason may be due to bigger cavity size of CB8, the interaction is not as strong as CB7.

Fluorescence study: The fluorescence spectra of PRODAN in presence and absence of CB_n are shown in Fig.2. In water, PRODAN exhibits emission maximum around 520nm due to intramolecular charge transfer (ICT).²¹ Here, charge transfer occurs from dimethylamino group to C=O group in the excited state. But after addition of cucurbituril (CB_n) this fluorescence intensity is getting quenched. The extent of quenching depends upon the size of the cucurbituril (i.e. 6, 7, or 8) which added in to the PRODAN aqueous solution. In presence of CB6, the fluorescence intensity is reduced slightly and indicates

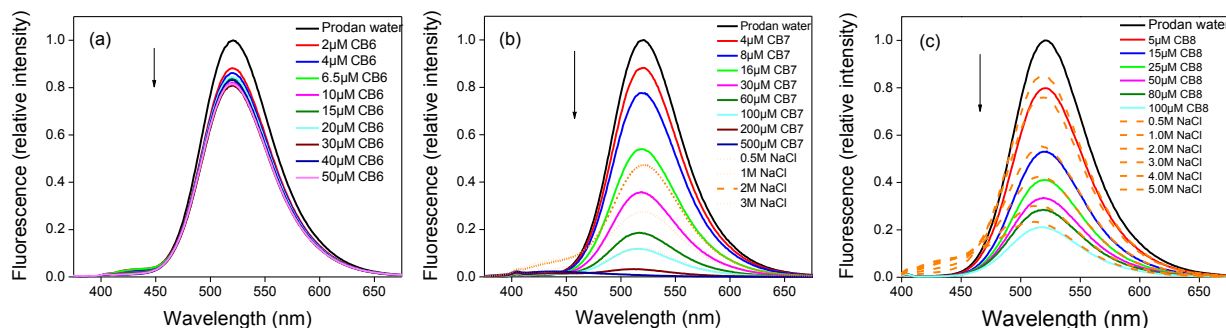


Fig.2 Fluorescence spectra of PRODAN in different concentration of (a) CB6, (b) CB7, (c) CB8, $\lambda_{ex}=355$ nm, $\lambda_{em}=520$ nm.

the absence of inclusion complexation between the PRODAN and CB6. For CB7 aqueous solution, dramatic changes occurred as shown in Fig.2 (b). The fluorescence intensity of PRODAN is completely vanished as CB7 concentration increases from 0 to 500×10^{-6} M. This shows strong interaction between PRODAN and CB7. For CB8 aqueous solution, the fluorescence intensity is reduced by 80% as shown in Fig.2 (c),

which may indicate that due to bigger cavity size of CB8, the interaction is not as strong as with CB7. These results clearly indicate that the charge transfer is getting restricted in the excited state in CB7 and CB8 cavity. According to Haridas pal,¹⁰ complexation of phenazine-based dye neutral red by CB7 is favored for the protonated amino group due to the ion-dipole interaction thereby accounting for the pKa shift towards higher values which causes the increased stability of the protonated dye in the complex. Therefore the dimethylamino group of PRODAN may be getting protonated due to increase in pKa value of amino group in CB7. The pKa value of dimethylamino group is 4.5 as given in the literature.²⁵ In water (about pH=7) this amino group is not getting protonated, following Henderson–Hasselbalch equation. But in CB7, this pKa value is increased; thereby amino group of PRODAN is getting protonated. This protonated PRODAN residing at the rim of cucurbituril macrocycle is further getting stabilized by ion-dipole interactions as we discussed earlier. Because of this partial positive charge on amino group, charge transfer from amino group to C=O group of PRODAN is restricted which

does not create any dipole moment in the excited state. This causes the fluorescence intensity to be quenched.

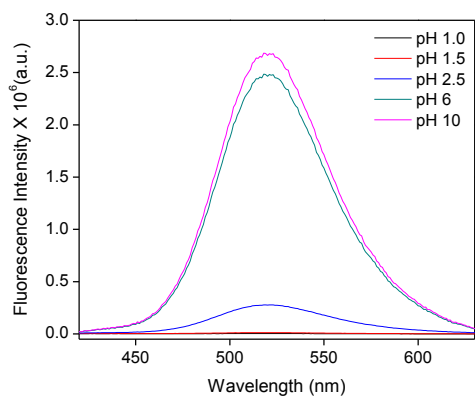


Fig.3 Fluorescence spectra of PRODAN in different pH, $\lambda_{ex}=355$ nm, $\lambda_{em}=520$ nm.

we know that the pKa value for protonation of amino group of PRODAN is 4.5. Therefore, below pH 4.5 the amino group is protonated which causes the restriction in the charge transfer from amino group to C=O group in PRODAN. In pH 6 and 10, the amino group is not protonated due to less pKa value of amino group than pH of solution. Therefore, pH dependent study further supports our conjuncture that dimethyl amino group of PRODAN is protonated in CBn cavity and stabilized by ion-dipole interactions.

Time-resolved measurements: Lifetime measurements of PRODAN monitored at $\lambda_{ex}=375\text{nm}$ in CB7 and CB8 are listed in Table 1 and 2 and fluorescence decay curves are shown in Fig.4. In 100×10^{-6} M concentration of CB7, lifetime value is slightly increased from 0.96 ns to 1.21 ns. And in the same CB8 concentration solution, change in lifetime value is almost negligible i.e. from 0.96 ns to 1.06 ns. So the increase in the lifetime value of PRODAN in CB7 is more than that in CB8 which indicates that the interaction between PRODAN and CB7 is more than that with CB8. But these small

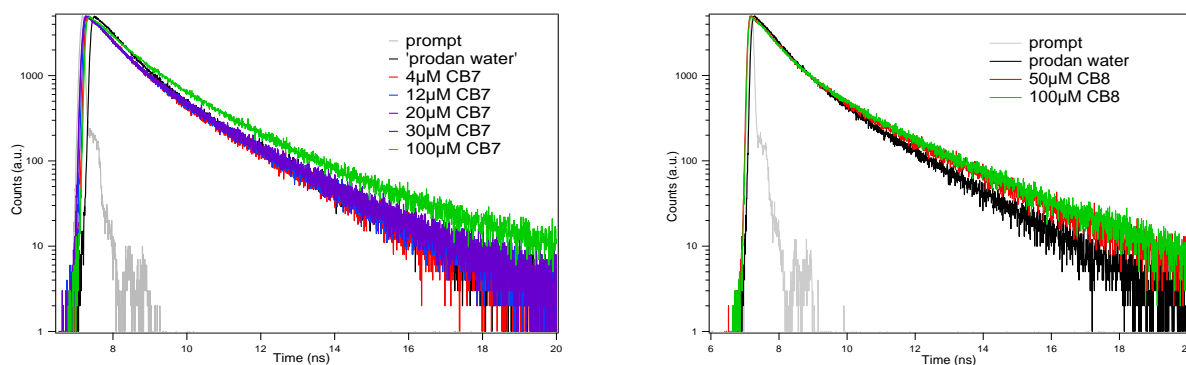


Fig.4 Fluorescence decay curves of PRODAN in water and in different concentration of (a) CB7, and (b) CB8, $\lambda_{ex}=375$ nm, $\lambda_{em}=520$ nm.

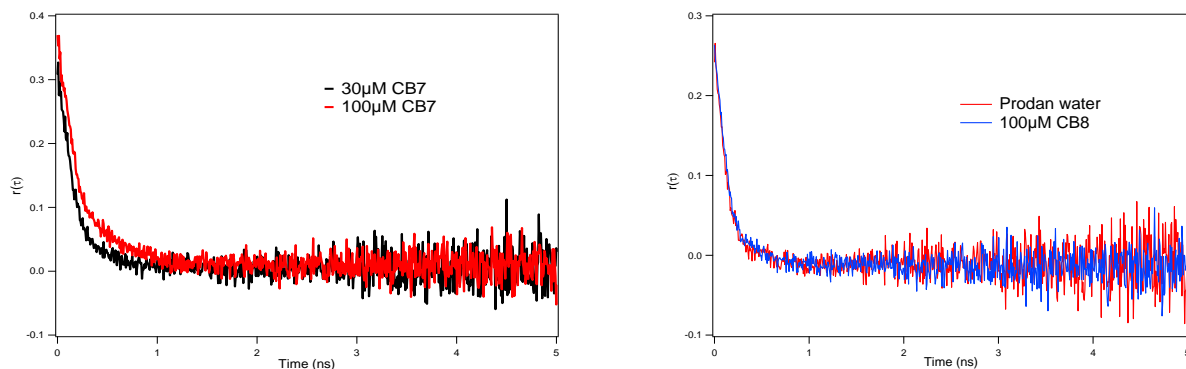


Fig.5 Fluorescence anisotropy decay curves of PRODAN in water and in different concentration of (a) CB7, and (b) CB8, $\lambda_{ex}=375$ nm, $\lambda_{em}=520$ nm.

increase in lifetime values shows that the interaction between PRODAN and CB7 is not strong. So PRODAN may be interacting with the CB7 and CB8 at its portal which causes minor decrement in non radiative decays.

Anisotropy study gives us information about how the rotational motions of PRODAN are restricted inside confined environment. Fig.5 shows anisotropy decay plots and their corresponding rotational relaxation time constant values are listed in

Table 3. Relaxation time constant for PRODAN in water is 0.14 ns and that in CB7 and CB8 (of 100 μ M concentration each) are 0.27 ns and 0.17 ns. Time constant value in CB7 is more than that in CB8 which indicates that the environment in CB7 is more rigid than in CB8.

Table 1. Fluorescence Decay Lifetimes of PRODAN in different CB7 concentration, λ_{ex} =375 nm, λ_{em} =520 nm.

Sample	τ_1 (ns) ^a	τ_2 (ns) ^a	B_1^a	B_2^a	R_1^a	R_2^a	τ_{av} (ns) ^a	χ^2
Prodan water	0.639	1.88	0.0529	0.0188	0.738	0.262	0.96	1.03621
CB7(20 μ M)	0.662	1.932	0.0445	0.0157	0.739	0.261	0.99	0.98596
CB7(100 μ M)	0.802	2.32	0.0539	0.0196	0.733	0.267	1.21	1.11636

(a = Experimental error \pm 5%)

Table 2. Fluorescence Decay Lifetimes of PRODAN in different CB8 concentration, λ_{ex} =375 nm, λ_{em} =520 nm.

Sample	τ_1 (ns) ^a	τ_2 (ns) ^a	B_1^a	B_2^a	R_1^a	R_2^a	τ_{av} (ns) ^a	χ^2
Prodan water	0.639	1.88	0.0529	0.0188	0.738	0.262	0.96	1.03621
CB8(25 μ M)	0.623	2.102	0.0587	0.018	0.765	0.235	0.97	1.02087
CB8(100 μ M)	0.659	2.38	0.0551	0.0169	0.765	0.235	1.06	1.10757

(a = Experimental error \pm 5%)

Table 3. Fluorescence Anisotropy Decay values of PRODAN in different CB7 & CB8 concentration, λ_{ex} =375 nm, λ_{em} =520 nm.

Sample	τ_1 (ns) ^a	τ_2 (ns) ^a	B_1^a	B_2^a	R_1^a	R_2^a	τ_{av} (ns) ^a	χ^2
prodan water	0.135	-	-	-	-	-	0.14	0.97473
CB7(30 μ M)	0.411	0.115	0.051	0.181	0.22	0.78	0.18	0.95
CB7(100 μ M)	0.397	0.061	0.124	0.076	0.62	0.38	0.27	0.97
CB8(50 μ M)	0.145	-	-	-	-	-	0.15	1.02479
CB8(100 μ M)	0.168	-	-	-	-	-	0.17	0.98765

(a = Experimental error \pm 5%)

To verify the interaction between PRODAN and CBn at its portal, we added NaCl in the PRODAN/ CB7 (& CB8) solution. So that positively charged Na⁺ ions bind to the C=O groups present at the portal of CB7 and CB8. After addition of NaCl in the aqueous solution, original fluorescence intensity (520 nm) is increased along with that a small peak at 430 nm also generated. PRODAN shows 430nm peak only in hydrophobic environment. So after addition of NaCl, Na⁺ ions replaces PRODAN molecule from the portal and now PRODAN molecule is going inside hydrophobic cavity of CB. Also

increase at 520nm peak indicates that PRODAN is now in bulk water. The increase in the fluorescence intensity is more at 520nm peak than that of 430nm peak. This is due to the repulsion between C=O group of PRODAN and C=O groups of CBs at its portal so that only few PRODAN molecules can enter inside CBn and most of them are remained in water. Fig.6 depicts the proposed structure of PRODAN:CBn complex which shows that the PRODAN molecule is not fully encapsulated by CBn but interacting at the portal.

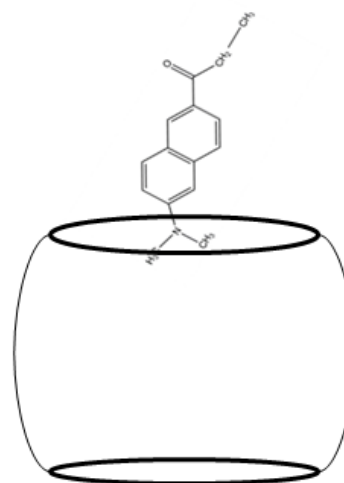
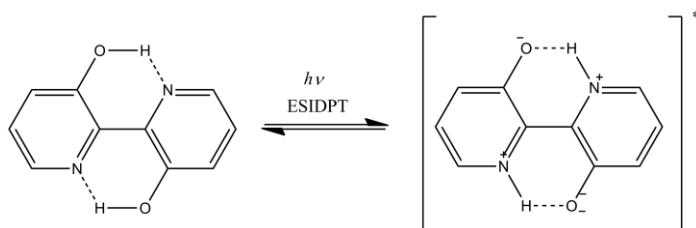


Fig.6 Proposed structure of PRODAN:CBn complex.

3.2. STUDY OF INTERACTION BETWEEN BIPYRIDINE DIOL [BP(OH)₂] and CUCURBITURIL

Molecules pursuing one or more hydrogen bonds in their structure are immensely important in photophysical studies. In the excited state, photo tautomerization occurs with these molecules and upon returning to the ground state, reverse tautomerization brings the molecule back to its original structure. Some



Scheme 5: [BP(OH)₂]

of these molecules have been suggested as a potential biological probe for the

study of protein conformation and binding sites, because of their extreme sensitivity to solvent polarity and hydrogen bonding with protic solvents.^{26,27} We propose one of such molecules, 2,2'-bipyridine-3,3'-diol [BP(OH)₂], which is a highly sensitive probe to microenvironment change. The photoinduced excited-state intramolecular double proton transfer (ESIDPT) occurs in BP(OH)₂ as shown in Scheme 5.²⁸ BP(OH)₂ exists in two forms, di-enol (DE) in the ground state and dizwitterion form (DZ) in the excited state.²⁸ Absorption and emission spectra and calculated excited state dipole moments show that the di-enol (DE) and dizwitterion (DZ) tautomers have negligible dipole moments.²⁸ BP(OH)₂ shows absorption peak in the region of 330-360 nm from DE form and additional peaks in the region of 400-450 nm from DZ form in water only.²⁹ Irrespective of excitation wavelength (DE or DZ), fluorescence is observed at 465 nm corresponding to DZ tautomer after an efficient ESIDPT process.²⁹

Datta et al.³⁰ have studied the binding of BP(OH)₂ with ionic and neutral surfactants like cetyltrimethylammonium bromide (CTAB), sodium dodecyl sulfate (SDS), and Triton X-100 (TX-100). They have shown that though all the three micelles have similar hydrophobic nanocavities, their binding interaction with BP(OH)₂ are different as revealed by the steady state and time resolved measurements. So depending upon hydrophobicity, local pH, viscosity and compactness of the micellar nanocavity, there is change in the fluorescence quantum yield of BP(OH)₂ and the

extent of ESIDPT. Such distinct spectral behavior of BP(OH)_2 towards polar and nonpolar environments can be utilized as both water sensor and biomarker.

Abou-Zied²⁹ has studied the ground and excited state tautomerization of the 2,2'-bipyridine-3,3'-diol molecule [BP(OH)_2] in different solvents and in confined nanocavities of cyclodextrins (CDs) using steady-state and lifetime spectroscopic measurements. In all solvents, a dizwitterion (DZ) tautomer is produced in the excited state after excited-state intramolecular double proton transfer (ESIDPT). In this paper, BP(OH)_2 has been used to probe the nanocavities of several cyclodextrins in aqueous solution that reflects the degree of hydrophobicity of the CD cavity and reveals the different mechanisms of probe encapsulation.²⁹

Our aim is to study spectral behavior of BP(OH)_2 in CBs which has similar hydrophobic cavity as that of CD but also hydrophilic carbonyl groups present on its portal. We have also used computational methods to get an idea of orientation of BP(OH)_2 in the inclusion complex.

RESULTS AND DISCUSSION

Absorption study: The absorption spectra of BP(OH)_2 in different concentration of CB6, CB7, and CB8 are shown in Fig.7 for the spectral region from 310-460 nm. The peak at 345 represents the transition to the lowest (π, π^*) state of dienol (DE)

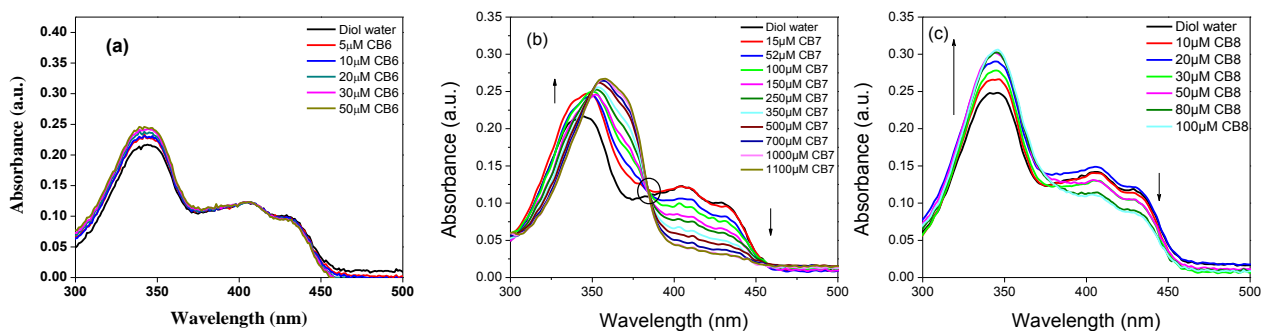


Fig.7 Absorption spectra of BP(OH)_2 in different concentration of (a) CB6, (b) CB7, (c) CB8.

tautomer.³¹ The double-peak absorption in the region 410-450 nm appears in water only.³² The double-peak absorption in the region 410-450 nm is from dizwitterion (DZ) tautomer and is stabilized in the ground state due to water solvation.³³ Due to presence of water molecules, the DZ tautomer is stabilized and the energy gap between the DE and DZ tautomer is reduced to just 3 kcal/mol.³³ Absorption spectra of BP(OH)₂ in presence of CBn are shown in Fig.7. In presence of CB6, the absorption spectra of BP(OH)₂ is similar with that of water which indicates the absence of any inclusion complex between BP(OH)₂ and CB6. For CB7 aqueous solution, as the concentration of CB7 increases, there is an increase in the intensity of the peak at 345 nm with a concomitant decrease in the intensity of the two peaks in the region 410-450 nm. This is due to the caging effect of the cucurbituril cavity on the guest molecule. Inside the CB due to hydrophobic cavity the dizwitterion (DZ) form gets converted to the dienol (DE) form which causes the decrease in the absorption intensity in the region 410-450 nm. In the case of CB8, this trend is somewhat small. Due to wide cavity size of CB8, the protection of BP(OH)₂ molecule from water is comparatively less than that in CB7. The absorption spectra of BP(OH)₂ in CB7 show a region at 384 nm where intersections occur, but in case of CB8 isosbestic points is not at all observed. Presence of isosbestic point indicates the presence of a single equilibrium between two species or two states.

Fluorescence study: Fig.8 and Fig. 9 depict the fluorescence spectra of BP(OH)₂ in different concentration of CB6, CB7, and CB8 excited at 345nm and 425 nm, respectively. In water fluorescence is coming from dizwitterion (DZ) tautomer due to ESIDPT.^{28-30,34} In Fig.8a and Fig.9a, there is no change in the fluorescence intensity of BP(OH)₂ after addition of CB6 indicating that there is no complex formation between BP(OH)₂ and CB6 due to smaller cavity size of CB6. In presence of CB7, the fluorescence intensity of BP(OH)₂ (Fig.8b) excited at 345 nm increases to 6 times compared to water, whereas the intensity excited at 425 nm (Fig.9b) decreases. For CB8 aqueous solution (Fig.8c) the increase in the fluorescence intensity is only 1.5 times compared to water, whereas that of intensity excited at 425 nm decreases as shown in Fig.9c. These results indicate that the binding interaction between of BP(OH)₂ and CB8 is not as strong as that of CB7, and it may be attributed to larger cavity size of

CB8 compared to CB7. The change in intensity upon excitation at 345 and 425 nm is well-correlated with that of absorption spectra. The reason behind increase in the fluorescence intensity excited at 345 nm is that inside the CB cavity vibrational and rotational motions of BP(OH)₂ are getting restricted, and thereby the non-radiative decay pathway of the molecule is severely inhibited. On the other hand, the decrease in

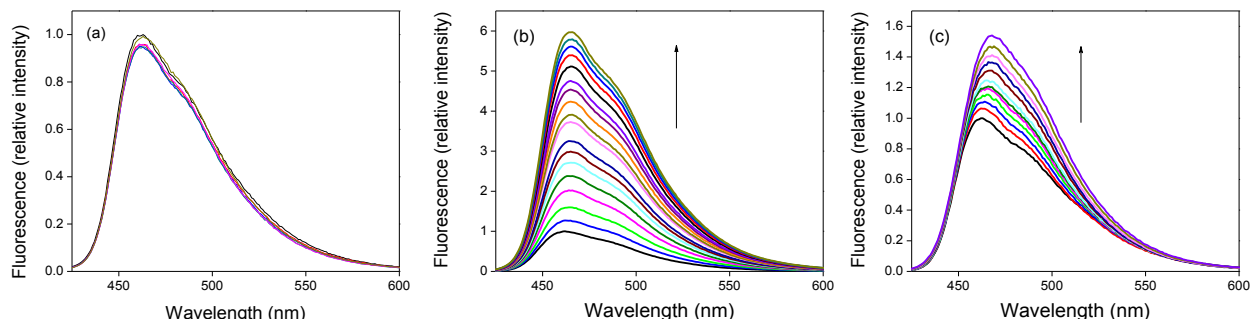


Fig.8 Fluorescence spectra of BP(OH)₂ in different concentration of (a) CB6 (0M to 50 μM), (b) CB7 (0M to 1100μM) and (c) CB8 (0M to 100μM), λ_{ex}=345 nm, λ_{em}=465 nm.

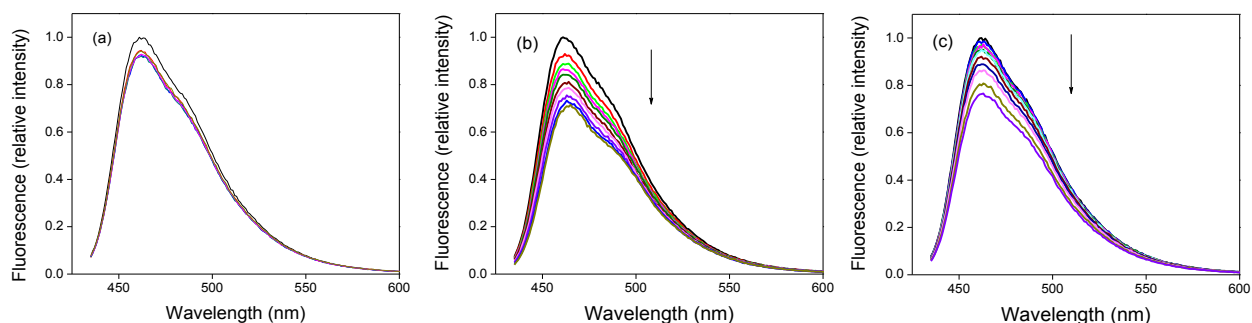


Fig.9 Fluorescence spectra of BP(OH)₂ in different concentration (a) CB6 (0M to 50 μM), (b) CB7 (0M to 1100μM) and (c) CB8 (0M to 100μM), λ_{ex}=425 nm, λ_{em}=465 nm.

fluorescence intensity excited at 425 nm peak, as CB7 concentration increases, is due to dizwitterion form getting converted to dienol form inside CB7 hydrophobic cavity. Therefore the absorbance at 425 nm decreases which shows the corresponding decrease in the fluorescence intensity. The stoichiometry ratios and binding constants were calculated with the help of Benesi-Hildebrand (BH)³⁵ double reciprocal plots as shown in Fig.10 using following equation.

$$\frac{1}{F - F_0} = \frac{1}{K(F_1 - F_0)[CB7]} + \frac{1}{F_1 - F_0}$$

The linearity of BH plot indicates the formation of 1:1 inclusion complex between BP(OH)_2 and CBn (for both CB7 and CB8). The estimated binding constant values are $2.66 \pm 0.1 \times 10^3 \text{ M}^{-1}$ and $1.81 \pm 0.1 \times 10^4 \text{ M}^{-1}$ for CB7 and CB8 . The reason may be the different orientation of BP(OH)_2 inside CB7 and CB8 as shown in Fig.13 and 14.

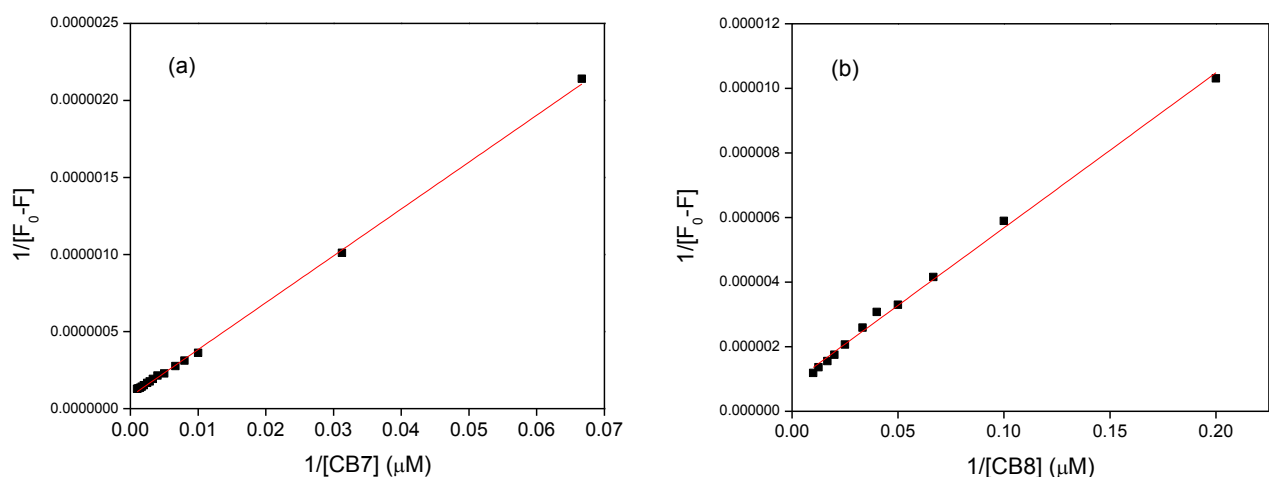


Fig.10 BH plots of BP(OH)_2 in (a) CB7 , and (b) CB8 .

To support these results fluorescence lifetime and anisotropy measurements were taken.

Time-resolved measurements: Fluorescence lifetime decay curves of BP(OH)_2 in presence and absence of CB6 , CB7 , and CB8 are shown in Fig.11. The lifetime results are listed in Table 4. Fluorescence lifetime of BP(OH)_2 in CB6 aqueous solution is 0.64

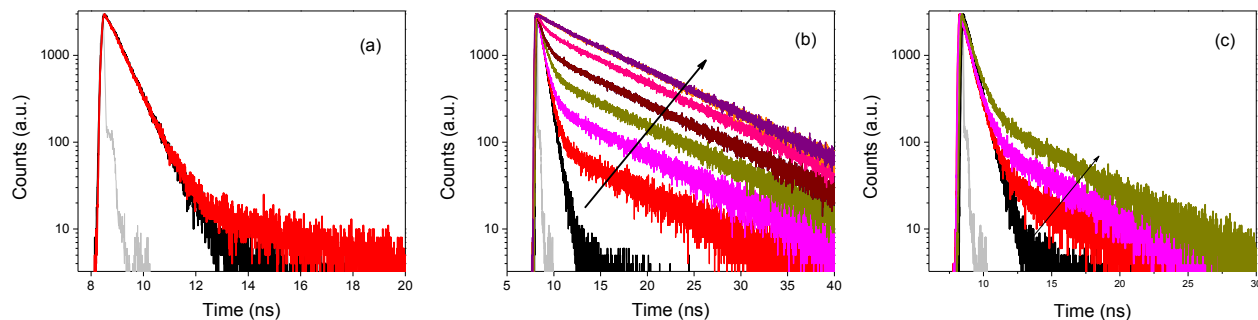


Fig.11 Fluorescence Decay curves of BP(OH)_2 in water and in increasing concentration of (a) CB6 (0M to 50 μM), (b) CB7 (0M to 1000 μM), (c) CB8 (0M to 100 μM), $\lambda_{\text{ex}}=375 \text{ nm}$, $\lambda_{\text{em}}=465 \text{ nm}$.

ns similar to that of Diol in water (0.633 ns), confirms there is no complex formation between BP(OH)₂ and CB6. In presence of CB7 the fluorescence lifetime of BP(OH)₂ increases (Fig.11 and Table 4) and at 1 mM of CB7 the lifetime was found to be 7.64 ns. In presence of 100 μM CB8 lifetime is 0.937 ns. When we compared this lifetime in presence of 100 μM CB7, it was found to be 1.93 ns. This suggests that the interaction between BP(OH)₂ and CB7 is stronger than that of CB8. Fluorescence anisotropy data is shown in Fig.12 and the fitting parameters are tabulated in Table 5. The rotational relaxation time (τ_r) of diol in water is 66.7 ps.

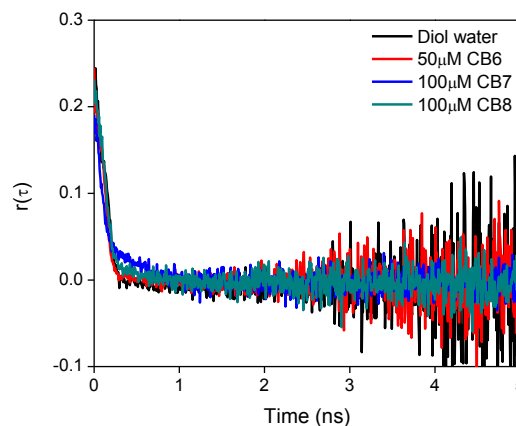


Fig.12 Fluorescence Anisotropy Decay curves of BP(OH)₂ in water and in different concentration of CB6, CB7, and CB8, $\lambda_{ex}=375$ nm, $\lambda_{em}=465$ nm.

In presence of CB6 τ_r was found to be 68.4 ps which are almost same, which confirms that diol doesn't form inclusion complex with CB6. In presence of CB7, τ_r is 352 ps, confirms the inclusion of diol with CB7 and in CB8 the value of τ_r is 126 ps. From this information it is clear that the rotational motion is more restricted inside CB7 than in CB8 and it is attributed to the formation of more rigid inclusion complex with CB7 than CB8.

Table 4. Fluorescence Decay values of BP(OH)₂ in water, and in different concentration of (a) CB6, (b) CB7, and (c) CB8 . $\lambda_{ex}=375$ nm, $\lambda_{em}=465$ nm. (a = experimental error \pm 5%)

Sample	τ_1 (ns) ^a	A_1 ^a	τ_2 (ns) ^a	A_2 ^a	τ_{av} (ns) ^a	χ^2
Diol-water	0.633	1			0.633	1.09
50μM CB6	0.597	0.99	4.821	0.01	0.64	1
100μM CB7	0.671	0.84	8.56	0.16	1.93	1.082
200μM CB7	0.683	0.63	8.65	0.37	3.63	0.9985
500μM CB7	0.686	0.25	8.74	0.75	6.69	1.03
1000μM CB7	0.686	0.13	8.71	0.87	7.64	1.016
20μM CB8	0.62	0.98	4.574	0.02	0.699	1.05
50μM CB8	0.61	0.96	4.65	0.04	0.771	1
100μM CB8	0.64	0.93	4.89	0.07	0.937	1.012

Table 5. Fluorescence anisotropy decay parameters of BP(OH)₂ in water, CB6, CB7, and CB8, λ_{ex} =375 nm, λ_{em} =465 nm.

Sample	Relaxation Time (τ_r in ps) ^a	χ^2
Water	66.7	1.18
CB6	68.4	1.09
CB7	352	0.99
CB8	126	1.19

Docking study:

To obtain a molecular picture of the orientation of BP(OH)₂ in the inclusion complexes with various CBs, as well as to gain insight into the stabilization achieved due to encapsulation, we have docked the ligand [BP(OH)₂] into the CBs. Fig.13 and 14 depict the structure of the most stable configuration of BP(OH)₂ embedded inside the CB7 and CB8 cavity. From these structures it is clear that diol, encaged inside CBn cavity is away from aqueous environment so that it can't undergo proton transfer to give dizwitterion form in the ground state. Docking results support our conjecture that CBn is protecting BP(OH)₂ from water and thus enhancing the proton transfer in excited state.

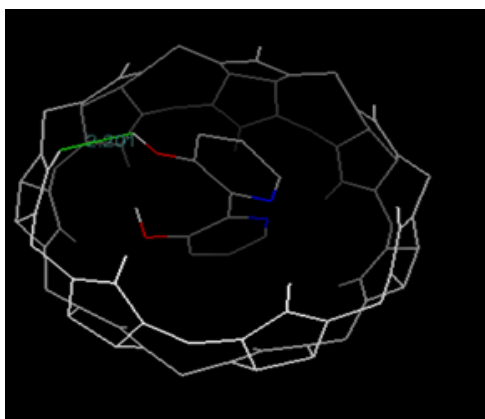


Fig.13 Structure of the most stable minimum configuration of BP(OH)₂ embedded inside the CB7 cavity.

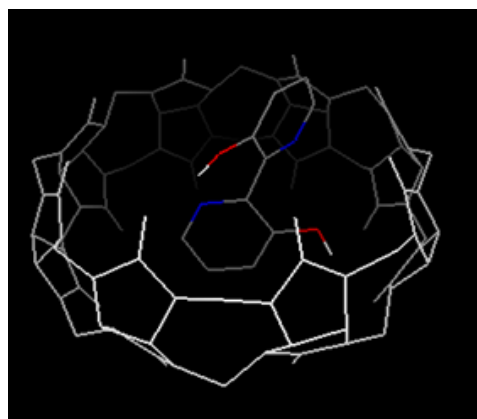
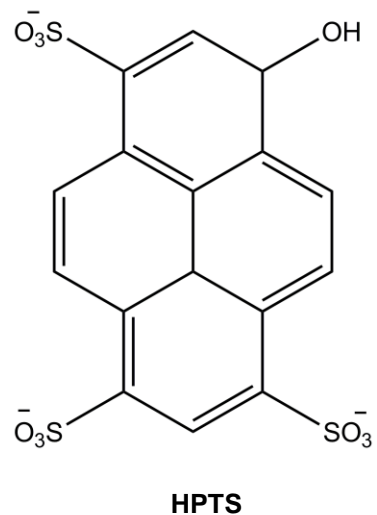


Fig.14 Structure of the most stable minimum configuration of BP(OH)₂ embedded inside the CB8 cavity.

3.3. STUDY OF INTERACTION BETWEEN HPTS and CUCURBITURIL

Proton transfer reaction plays very important role in many biological and chemical processes³⁶ e.g. in transport of proton through membrane and abnormally high mobility of proton in water.³⁷ Excited state proton transfer (ESPT) in organized assemblies and in bulk liquid solutions gives important information about the nature and mechanism of acid-base reactions.³⁶ Ground and excited state proton transfer reactions of HPTS (8-hydroxypyrene-1,3,6-trisulfonate, pyranine) have been studied in water,³⁸ liquid mixtures³⁹, micelle⁴⁰, reverse micelle⁴¹, and biomolecules⁴². The pKa value of HPTS is 7.4 in the ground state and decreases to 0.4 in the first excited state.⁴³ ESPT from HPTS to water basically consists of three steps – proton transfer, recombination, and dissociation.⁴⁴ Due to faster process of recombination, the dissociation of the acid is much more slower than the initial proton transfer step.⁴⁴ In water, at low pH(<7) HPTS shows absorption at 405 nm due to protonated (ROH) form and at a high pH(>8) shows absorption peak at 450 nm which corresponds to deprotonated (RO⁻) form.⁵⁰ HPTS exhibits fluorescence emission at 435 nm due to protonated (ROH) form and at 515 nm due to deprotonated (RO⁻) form.³⁷



Huppert et al.⁴⁵ have studied the effect of electrolytes (MgCl₂ and NaCl) on the rate of proton transfer from HPTS to water. They suggested that depending upon the number of free water molecules present around the HPTS molecule, the proton transfer reaction occurs. In absence of any salt in water, proton is rapidly transferred to a water cluster of more than 10 water molecules. But in the presence of salt, due to strong electrostatic/ hydrogen bond interaction, a large fraction of water molecules remain bound to the ion. Therefore, the amount of free water molecules decreases and this is the reason for the retardation of ESPT.

Mondal et al.⁴⁶ have studied ESPT of HPTS in niosome (surfactant vesicles). They have shown that the time constant for proton transfer, recombination, and dissociation in a niosome is 2 to 8 times slower than in bulk water. The reason for this is shielding of HPTS, slower solvation, slower diffusion of RO⁻, lower dielectric constant and higher friction inside a niosome compared to bulk water.

Similarly Bhattacharya et al.⁴⁴ have proved that ESPT of HPTS is slowed down inside γ -cyclodextrin cavity. However, in order to understand how the ESPT process is getting affected inside the cavity, it is necessary to carry out the excited state photophysics in some other nanocavity. With this aim, our present study mainly focuses on how ESPT process is getting affected inside hydrophobic cucurbituril (CB8) cavity having hydrophilic carbonyl groups present in its portal.

RESULTS AND DISCUSSION

Absorption study: The absorption spectra of HPTS in absence and presence of CB8 are shown in Fig. 15. Here it is pertinent to mention that the pKa value of -OH group of HPTS is 7.4.⁴⁴ As the experiment is carried out at pH 7.4 buffer solution, hence the absorption peak at 405 nm due to protonated (ROH) form and at 455 nm due to deprotonated (RO⁻) form.³⁶ Due to bigger molecular size of HPTS, CB7 cannot encapsulate the HPTS molecule but CB8 can encapsulate HPTS. As the CB8 concentration increases the absorption intensity of both peaks reduces and a new peak is generating at 490 nm. The absorption spectra clearly indicate that the strong interaction is going on between HPTS and CB8.

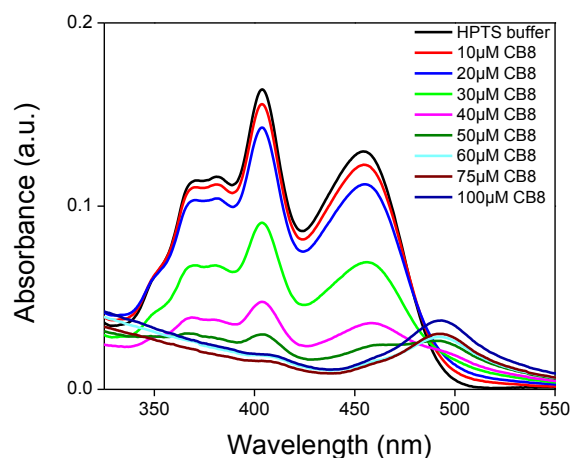


Fig.15 Absorption spectra of HPTS in different concentration of CB8.

Fluorescence study: Fig.16 depicts fluorescence spectra of HPTS in different concentration of CB8 excited at 405 and 455 nm. The fluorescence spectra of HPTS shows peak at around 515 nm and the fluorescence intensity is getting quenched as

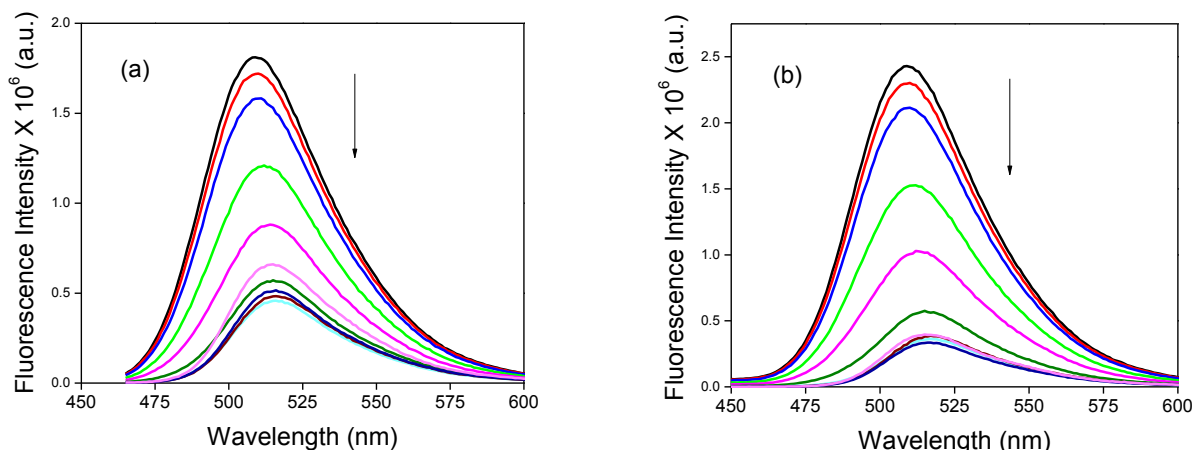


Fig.16 Fluorescence spectra of HPTS in different concentration of CB8, (a) $\lambda_{ex}=405$ nm (0M to 100 μ M), and (b) $\lambda_{ex}=455$ nm (0M to 100 μ M), $\lambda_{em}=515$ nm.

CB8 concentration increases. Generally, there is an enhancement in fluorescence intensity after a dye binding to host cavity, due to retardation of non radiative pathways inside CB8 cavity. In the present system, fluorescence quenching is an unusual observation. We propose the reason for this quenching is the restriction of excited state proton transfer (ESPT) due to hydrogen bonding between –OH group of HPTS and carbonyl groups of CB8 present at the portal. There are examples in the literature that indicates that fluorescence quenching is mainly due to some specific interactions like hydrogen bonding, charge transfer, etc.^{47,48} The stoichiometry was calculated with the help of Benesi-Hildebrand

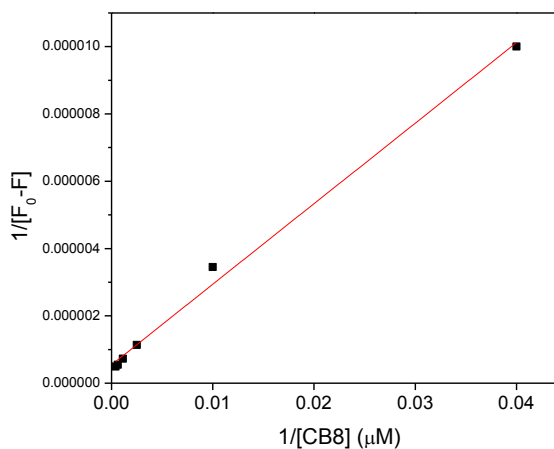


Fig.17 BH plot of HPTS in CB8.

(BH) reciprocal plots as shown in Fig.17. From BH plot, it is clear that stoichiometry is 1:1 for HPTS and CB8 complex, and the binding constant is estimated to be 2.275×10^3 .

Time-resolved measurements: Fluorescence decays of HPTS in presence and absence of CB8 are shown in Fig.18 and fitting parameters are tabulated in Table 6. In

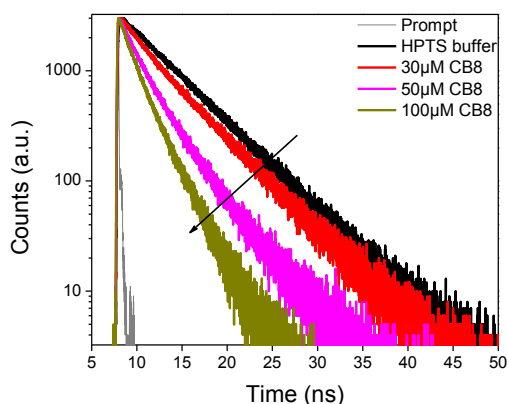


Fig.18 Fluorescence Decay curves of HPTS in different concentration of CB8, $\lambda_{ex}=375$ nm, $\lambda_{em}=515$ nm

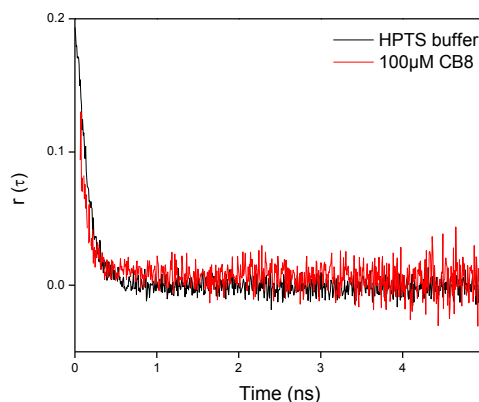


Fig.19 Fluorescence Anisotropy Decay curves of HPTS in water and in 100 μ M conc. of CB8, $\lambda_{ex}=375$ nm, $\lambda_{em}=515$ nm.

blank water, HPTS exhibits biexponential decay with an average lifetime of 3.7 ns. With gradual addition of CB8, the average decreases. This decreased lifetime value may be attributed to restriction in the ESPT due to hydrogen bonding interaction between HPTS and CB8 portal.⁵³ From anisotropy data (Fig.19), the rotational relaxation time in buffer and in presence of $100 \pm 0.1 \times 10^{-6}$ M CB8 concentration are 0.141 ns and 3.25 ns, respectively. The anisotropy results clearly infer that in the inclusion complex the free rotational motion of HPTS is restricted inside CB8 cavity.

Table 6. Fluorescence Lifetime Decay values of HPTS in different concentration of CB8 aqueous solution, $\lambda_{ex}=375$ nm, $\lambda_{em}=515$ nm.

Sample	A_1^a	τ_1 (ns) ^a	A_2^a	τ_2 (ns) ^a	τ_{av} (ns) ^a	χ^2
buffer	-0.32	0.151	0.68	5.38	3.7	1.103
50 μ M CB8	0.63	1.84	0.37	4.11	2.68	1.044
75 μ M CB8	0.45	1.35	0.55	2.95	2.23	1.05
100 μ M CB8	0.48	1.18	0.52	2.62	1.92	0.997

(a = experimental error \pm 5%)

Docking study:

To obtain a molecular picture of the orientation of HPTS in the inclusion complexes with various CBs, as well as to gain insight into the stabilization achieved due to encapsulation, we have docked the ligand HPTS into the CBs. The resulted HPTS:CB8 inclusion complex is shown in Fig.20. Hydroxyl group of HPTS forms hydrogen bond with carbonyl portal of CB8. This might be the reason for the restriction of excited state proton transfer (ESPT) of HPTS. Docking results support the experimental findings.

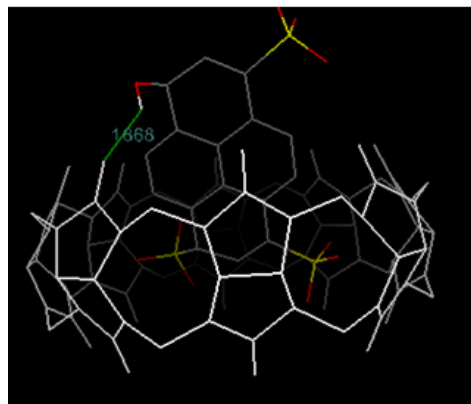


Fig.20 Structure of the most stable minimum configuration of HPTS embedded inside the CB8 cavity.

4. CONCLUSIONS

In the present work, the interaction behavior of PRODAN, Bipyridine Diol, and Pyranine (HPTS) with the cucurbituril (CBn) host have been studied with the help of absorption, steady state emission and time resolved measurements.

In PRODAN case, quenching in fluorescence is observed due to restriction of intramolecular charge transfer (ICT) process. This is due to dimethyl amino group of PRODAN is getting protonated due to increase in its pKa value and this positive charge is stabilized by electron rich carbonyl groups present at the portal of CB7. From time resolved studies we observed that in PRODAN:CB7 complex, PRODAN molecule is not fully encapsulated by the CB7 cavity but interacting at the portal through ion-dipole interactions.

Interaction of BP(OH)₂ with cucurbiturils was studied using absorption and fluorescence spectroscopy. The absorption of BP(OH)₂ molecule in water shows broad peak in the region of 400-450 nm due to stabilization of dizwitterion tautomer in the ground state. The fluorescence intensity of BP(OH)₂, when excited at 345 nm, increases after addition CB and decreases when excited at 425 nm. Also due to rigid environment inside CB cavity, rotational motions are restricted which restricts non-radiative decay and causes enhancement in the fluorescence intensity. These restrictions can be confirmed by lifetime and anisotropy data. Lifetime and anisotropy values of BP(OH)₂ is increased after gradual addition of CB7 and CB8 which indicates the more rigid environment inside CB cavity. Docking studies were employed to find the minimized inclusion complex of diol with CBn (7 and 8).

In case of HPTS, the fluorescence emission is quenched after addition of CB8. This quenching is attributed to the restriction of excited state proton transfer (ESPT) due to hydrogen bonding present between –OH group of HPTS and carbonyl groups of CB8 at the portal. The decrease in fluorescence lifetime in presence of CB8 also supports the hydrogen bonding interaction. Docking structure of inclusion complex HPTS with CB8 confirms the hydrogen bonding interaction between them.

REFERENCES

1. Lakowicz, J.R.; "Principles of Fluorescence Spectroscopy", 3rd edition, *Springer Science: New York, USA*, **2006**.
2. Schramm, M.; Hooley, R.; Julius, R.; "Guest Recognition with Micelle-Bound Cavitands", *J. Am. Chem. Soc.*, **2007**, *129*, 9773.
3. Fendler, J.; "Atomic and Molecular Clusters in Membrane Mimetic Chemistry", *Chem. Rev.*, **1907**, *87*, 877.
4. Dsouza, R.; Pischel, U.; Nau, W. M.; "Fluorescent Dyes and Their Supramolecular Host/Guest Complexes with Macrocycles in Aqueous Solution", *Chem. Rev.* **2011**, *111*, 7941.
5. Rekharsky, M. V.; Inoue, Y.; "Complexation Thermodynamics of Cyclodextrins", *Chem. Rev.*, **1998**, *98*, 1875.
6. Artiss, J.D.; Brogan, K.; Brucal, M.; Moghaddam, M.; Jen, K.L.C.; "The effects of a new soluble dietary fiber on weight gain and selected blood parameters in rats", *Metabolism*, **2006**, *55*, 195.
7. Shinkai, S.; Mori, S.; Koreishi, H.; Tsubaki, T.; Manabe, O.; "Hexasulfonated calix[6]arene derivatives: a new class of catalysts, surfactants, and host molecules", *J. Am. Chem. Soc.*, **1986**, *108*, 2409.
8. Zhu, W.; Gou, P.; Shen, Z.; "Applications of Calixarenes in Polymer Synthesis", *Macromolecular Symposia*, **2008**, *261*, 74.
9. Behrend, R.; Meyer, E.; Rusche, F.; Liebigs, *Ann. Chem.*, **1905**, 339, 1.
10. Mohanty, J.; Bhasikuttan, A.; Nau, W. M.; Pal, H.; "Host-Guest Complexation of Neutral Red with Macrocyclic Host Molecules: Contrasting p*K*_a Shifts and Binding Affinities for Cucurbit[7]uril and β -Cyclodextrin", *J. Phys. Chem. B*, **2006**, *110*, 5132.
11. Marquez, C.; Huang, F.; Nau, W. M., *Trans. Nanobiosci.*, **2004**, *3*, 39.

12. Walker, S.; Oun, R.; McInnes, F.; Wheate, N. J.; "The Potential of Cucurbit[n]urils in Drug Delivery", *Israel J. Chem.*, **2011**, *51*, 616.
13. Mohanty, J.; Nau, W. M.; "Ultrastable Rhodamine with Cucurbituril", *Angew. Chem., Int. Ed.* **2005**, *44*, 3750.
14. Nau, W. M.; Greiner, G.; Wall, J.; Rau, H.; Olivucci, M.; Robb, M. A.; "The Mechanism for Hydrogen Abstraction by n,π^* Excited Singlet States: Evidence for Thermal Activation and Deactivation through a Conical Intersection", *Angew. Chem., Int. Ed.*, **1998**, *37*, 98.
15. Lau, V.; Heyne, B.; "Calix[4]arene sulfonate as a template for forming fluorescent thiazoleorange H-aggregates", *Chem. Commun.*, **2010**, *46*, 3595.
16. Gavval, K.; Sengupta, A.; Hazra, P.; "Modulation of Photophysics and pKa Shift of the Anti-cancer Drug Camptothecin in the Nanocavities of Supramolecular Hosts", *Chem. Phys. Chem.*, **2013**, *14*, 532.
17. Catalan, J.; Perez, P.; Laynez, J.; Blanco, F. G.; "Analysis of the solvent effect on the photophysics properties of 6-propionyl-2-(dimethylamino)naphthalene (PRODAN)", *J. Fluor.*, **1991**, *1*, 215.
18. Krasnowska, E. K.; Gratton, E.; Parasassi, T.; "Prodan as a membrane surface fluorescence probe: partitioning between water and phospholipid phases", *Biophys J.*, **1998**, *74*, 1984.
19. Rottenberg, H.; "Probing the interactions of alcohols with biological membranes with the fluorescent probe Prodan", *Biochemistry*, **1992**, *31*, 9473.
20. Weber, G.; Farris, F.; "Synthesis and spectral properties of a hydrophobic fluorescent probe: 6-propionyl-2-(dimethylamino)naphthalene (PRODAN)", *Biochemistry*, **1979**, *18*, 3075.
21. Al-Hassan, K.; Khanfer, M.; "Fluorescence Probes for Cyclodextrin Interiors", *J. Fluor.*, **1998**, *8*, 19.

22. Bunker, C.; Bowen, T.; Sun, Y.; "A Photophysical Study of Solvatochromic Probe 6-Propionyl-Z(N,N-Dimethylamino) Naphthalene (PRODAN) in Solution", *Photochem. Photobiol.* **1993**, *58*, 499.
23. Samanta, A.; Fessenden, R.; "Excited State Dipole Moment of PRODAN as Determined from Transient Dielectric Loss Measurements", *J. Phys. Chem. A*, **2000**, *104*, 8972.
24. Adhikary, R.; Barnes, C.; Petrich, J.; "Solvation Dynamics of the Fluorescent Probe PRODAN in Heterogeneous Environments: Contributions from the Locally Excited and Charge-Transferred States", *J. Phys. Chem. B*, **2009**, *113*, 11999.
25. Chong, P.; Capes, S.; Wong, P.; "Effects of Hydrostatic Pressure on the Location of PRODAN in Lipid Bilayers: A FT-IR Study", *Biochemistry*, **1989**, *28*, 8358.
26. Sytnik, A.; Gormin, D.; Kasha, M.; "Interplay between excited-state intramolecular proton transfer and charge transfer in flavonols and their use as protein-binding-site fluorescence probes", *PNAS*, **1994**, *91*, 11968.
27. Sytnik, A.; Kasha, M.; "Excited-state intramolecular proton transfer as a fluorescence probe for protein binding-site static polarity", *PNAS*, **1994**, *91*, 8627.
28. Abou-Zied, O.; "Investigating 2,2'-Bipyridine-3,3'-diol as a Microenvironment-Sensitive Probe: Its Binding to Cyclodextrins and Human Serum Albumin", *J. Phys. Chem. B*, **2007**, *111*, 9879.
29. Abou-Zied, O.; "Steady-State and Time-Resolved Spectroscopy of 2,2'-Bipyridine-3,3'-diol in Solvents and Cyclodextrins: Polarity and Nanoconfinement Effects on Tautomerization", *J. Phys. Chem. B*, **2010**, *114*, 1069.
30. Dipanwita, D.; Datta, A.; "Modulation of Ground and Excited-State Dynamics of [2,2'-Bipyridyl]-3,3'-diol by Micelles", *J. Phys. Chem. B*, **2011**, *115*, 1032.
31. Bulska, H.; "Intramolecular cooperative double proton transfer in [2,2'-bipyridyl]-3,3'-diol", *Chem. Phys. Lett.*, **1983**, *98*, 398.

32. Carballeir, L.; Perez-Juste, I.; "Influence of water in the tautomerism of 2,2'-bipyridine-3,3'-diol", *J. Mol. Struct. (Theochem)*, **1996**, 368 17.
33. Barone, V.; Palma, A.; Sanna, N.; "Towards a reliable computational support to the spectroscopic characterization of excited state intramolecular proton transfer: [2,2'-bipyridine]-3,3'-diol as a test case", *Chem. Phys. Lett.*, **2003**, 381,451.
34. Sobolewska, A.; Adamowicz, L.; "Double-proton-transfer in [2,2'-bipyridine]-3,3'-diol: an ab initio study", *Chem. Phys. Lett.*, **1996**, 252, 33.
35. Benesi, H.; Hildebrand, J. H.; "A Spectrophotometric Investigation of the Interaction of Iodine with Aromatic Hydrocarbons", *J. Am. Chem. Soc.*, **1949**, 71, 2703.
36. Mondal, S.; Sahu, K.; Ghosh, S.; Sen, P.; Bhattacharyya, K.; "Excited-State Proton Transfer from Pyranine to Acetate in γ -Cyclodextrin and Hydroxypropyl γ -Cyclodextrin", *J. Phys. Chem. A*, **2006**, 110, 13646.
37. Agmon, N.; Elementary Steps in Excited-State Proton Transfer, *J. Phys. Chem. A*, **2005**, 109, 13.
38. Tran-thi, T.; Gustavsson, T.; Prayer, C.; Pommeret, S.; Hynes, J.; "Primary ultrafast events preceding the photoinduced proton transfer from pyranine to water", *Chem. Phys. Lett.*, **2000**, 329, 421.
39. Agmon, N.; Huppert, D.; Masad, D.; Pines, D.; "Excited-state proton transfer to methanol-water mixtures", *J. Phys. Chem.*, **1991**, 95, 10407.
40. Politi, M.; Fendler, J.; "Laser pH-jump initiated proton transfer on charged micellar surfaces", *J. Am. Chem. Soc.*, **1984**, 106, 265.
41. Politi, M.; Brandt, O.; Fendler, J.; "Ground- and excited-state proton transfers in reversed micelles, polarity restrictions and isotope effects", *J. Phys. Chem.*, **1985**, 89, 2345.
42. Nachliel, E.; Gutman, M.; Kiryati, S.; Dencher, N.; "Protonation dynamics of the extracellular and cytoplasmic surface of bacteriorhodopsin in the purple membrane", *Proc. Natl. Acad. Sci.*, **1996**, 93, 10747.

43. Smith, K.; Kaufmann, K.; Huppert, D.; Gutman, M.; "Picosecond proton ejection: an ultrafast pH jump", *Chem. Phys. Lett.*, **1979**, *64*, 522.
44. Mondal, S.; Sahu, K.; Sen, P.; Roy, D.; Ghosh, S.; Bhattacharyya, K.; "Excited state proton transfer of pyranine in a γ -cyclodextrin cavity", *Chem. Phys. Lett.*, **2005**, *412*, 228.
45. Leiderman, P.; Gepshtein, R.; Uritski, A.; Genosar, L.; Huppert, D.; "Effect of Electrolytes on the Excited-State Proton Transfer and Geminate Recombination", *J. Phys. Chem. A*, **2006**, *110*, 5573.
46. Mondal, T.; Ghosh, S.; Das, A.; Mandal, A.; Bhattacharyya, K.; "Salt Effect on the Ultrafast Proton Transfer in Niosome", *J. Phys. Chem. B*, **2012**, *116*, 8105.
47. Shaikh, M.; Mohanty, J.; Sundararajan, M.; Bhasikuttan, A.; Pal, H.; "Supramolecular Host-Guest Interactions of Oxazine-1 Dye with β - and γ -Cyclodextrins: A Photophysical and Quantum Chemical Study", *J. Phys. Chem. B*, **2012**, *116*, 12450.
48. Reija, B.; Al-Soufi, W.; Novo, M.; Tato, J. V.; "Specific Interactions in the Inclusion Complexes of Pyronines Y and B with β -Cyclodextrin", *J. Phys. Chem. B*, **2005**, *109* (4), 1364.